Power Line Communication for Low-Bandwidth Control and Sensing

Adedayo O. Aderibole ⓘ, Erik K. Saathoff ⓘ, *Graduate Student Member, IEEE*, Kevin J. Kircher ⓘ, Steven B. Leeb ⓘ, *Fellow, IEEE*, and Leslie K. Norford ⓘ

Abstract—While not designed with communication applications in mind, power lines have been attractive targets for providing ancillary communication services for decades. Unfortunately, loads and switchgear can easily interfere with reliable communication in both direct and subtle ways. Power line communication (PLC) is therefore often relegated to non-critical control tasks like home lighting or appliance control, where communication difficulties or failure simply result in a walk to the light switch. For control applications that require low data rates, unexploited opportunities exist for increasing the reliability of PLC within governing regulatory rules. Reliable, low-bandwidth PLC facilitates new, inexpensive opportunities for demand-side management of the loads in a building or facility. This paper presents approaches for tailoring PLC for reliable low-bandwidth communication, and presents experimental demonstrations in a 24-floor high-rise building with challenging channel conditions.

Index Terms—Binary orthogonal keying, chirp spread spectrum, low-bandwidth communication, power line communication, quasi-peak.

I. BACKGROUND

ENERGY conservation and management schemes based on demand response typically require a communication channel [1]. Communication requirements often add expense, and may limit the penetration and efficacy of demand response or load control schemes. Effective communication is necessary not only to save energy and shave peak demand, but also to ensure the reliability of essential services such as hot water, air conditioning, and vehicle charging.

Existing power lines already connect loads to utility control centers and to each other. For this reason, power lines are a potentially attractive communication channel for demand response applications. While power lines were not designed for communication [2], attempts have been made for decades. Power-line communication (PLC) was originally employed by power utility companies in the 1920 s for long distance communication, remote monitoring, protection, and control of equipment on the utility grid [3]. Smart grids demand bi-directional communication, inter-connectivity, and the intelligent automation of components on the electrical power network [4]. PLC systems suitable for smart-grid applications such as load and peak demand management are frequently proposed [5], and PLC may also provide a route to protect against cyberattacks and extreme environmental concerns [6].

Time-varying noise levels and poorly characterized line impedance, especially as loads connect and disconnect from the line, are major issues that affect the practical application of PLC. Power line noise may be synchronous or asynchronous with respect to the line-cycle, and may include colored background and impulse noise [7], [8]. Power line noise is difficult to characterize and is not easily approximated as additive white Gaussian noise [7]. Unpredictable signal attenuation, dependent on the time of day, frequency, distance, and electrical phase, deteriorates the received signal power in PLC systems [9]. Network topology, multipath fading, and circuit loading also influence attenuation [10]. The achievable performance of PLC systems is limited by impedance, bandwidth and electromagnetic compatibility (EMC) constraints [11] enforced by regulatory bodies such as the Federal Communications Commission (FCC) in the United States and Comité Européen de Normalisation Électrotechnique (CENELEC) in Europe [7].

Smart grid and demand response applications may have relatively unique communication requirements that can be exploited to improve the utility of PLC for control and monitoring. Specifically, many demand response and control applications require far lower bandwidths than other consumer applications of PLC like internet or land-line phone extenders. Communication bandwidths of a few Hertz or less may be adequate for many control applications. This paper presents a suite of techniques that can substantially enhance PLC communication reliability by taking advantage of the unique requirements imposed by low-bandwidth communication. The proposed techniques leverage the "quasi-peak" (QP) regulations to improve the reliability of low-bandwidth PLC using chirp signals. This paper also proposes methods and hardware to take advantage of this opportunity and substantially improve PLC reliability in low-bandwidth applications. Section III presents a review of relevant PLC regulatory requirements, followed by an opportunity to leverage the so-called QP regulations to improve communication in low-bandwidth applications. Section IV

Adedayo O. Aderibole, Erik K. Saathoff, Kevin J. Kircher, and Steven B. Leeb are with the Electrical Engineering and Computer Science Department, Massachusetts Institute of Technology, Cambridge, MA 02139 USA (e-mail: adedayo@mit.edu; saathoff@mit.edu; kircher@mit.edu; sbleeb@mit.edu).

Leslie K. Norford is with the Department of Architecture, Massachusetts Institute of Technology, Cambridge, MA 02139 USA (e-mail: lnorford@mit.edu).

discusses the modulation and demodulation schemes required to utilize the QP opportunity. These techniques are then applied to the design and implementation of new PLC modem hardware to exploit the opportunity in Section V. Section VI describes a 24-floor high-rise building used as a test environment to evaluate the proposed techniques and hardware. The experimental results obtained in the test building are presented in Section VII.

II. PLC SYSTEMS

PLC systems are usually classified according to the frequency band in which they operate. Ultra-narrowband (UNB-PLC), narrowband (NB-PLC) and broadband (BB-PLC) operate in the 125 Hz-3-kHz, 3-500-kHz, and 1.8-100-MHz spectrum, respectively [5]. NB-PLC is attractive for smart grid applications where reliability, coverage and robustness are the main concern, while BB-PLC is mainly employed in internet access applications for home and building area networks with limited range [12]. Electromagnetic interference (EMI) regulations set the conducted and radiated emissions limits which determine the maximum transmitted communication signal power level for UNB-PLC, NB-PLC and BB-PLC systems. CENELEC defines the 3-148.5-kHz spectrum only for NB-PLC with conducted emissions constraints provided in European Norms (EN) 50065-1 [13] in the form of peak, quasi-peak and average limits. EN 50065-1 does not provide radiation emissions limits for NB-PLC. In the United States, the FCC Part 15 [14] specifies the 9-490-kHz spectrum for NB-PLC applications. However, no in-band conducted emissions limits are provided. Radiated emissions limits for NB-PLC are provided by the FCC in [14]. In addition, non-regulatory bodies such as the Comité International Spécial des Perturbations Radioélectriques (CISPR) and IEEE have proposed emission limits for NB-PLC in the 9–500-kHz spectrum in the CISPR 22 [15] and IEEE 1901.2 [16] standards, respectively.

In addition to EMI, PLC signals should be below certain limits to ensure the safety of equipment on the utility grid and operators. IEEE Standard (Std.) 519-2014 states that the voltage harmonics content at the interface between users in a system should be below the limits provided in [17]. Consequently, the total conducted emissions of PLC devices in a network should be such that the recommended voltage harmonics levels at the point of common coupling are not violated. Furthermore, periodic PLC signals can cause voltage or current surges that lead to equipment damage as stated in IEEE C62.41 [18]. The lower voltage limit surge protection equipment is able to withstand is 500 V [18]. PLC signals should thus be kept far below this limit for safety. Finally, residual current devices at service panels activate in the presence of excessive common-mode current. To avoid tripping these devices, common-mode currents from PLC modems should respect the 30-mA limit specified in IEC 60755 [19].

Despite the many challenges facing PLC, many researchers have highlighted the benefits of PLC in smart grid applications. In [20], PLC was employed to create a network in a smart home for Internet of Things (IoT) applications. In [20], a BB-PLC system provided internet access to the IoT network. Advanced

TABLE I
CONDUCTED EMISSIONS LIMITS FOR NB-PLC

Frequency Range	P (dBμV)	QP (dBμV)	AV (dBμV)
3 kHz - 9 kHz [1]	134	-	-
9 kHz - 95 kHz [1]	134 - 120[2]	-	-
95 kHz - 148.5 kHz [1]	134[3]/122[4]	-	-
150 kHz - 500 kHz [5]	-	115 - 105[2]	105 - 95[2]

[1] CENELEC EN 50065-1 regulatory limits.
[2] Decreases linearly with the logarithm of frequency.
[3] Limit for Class A (industrial-use) devices.
[4] Limit for Class B (general-use) devices.
[5] Recommended by IEEE in IEEE Std. 1901.2.

metering infrastructure that enables two-way information exchange using PLC between utilities and consumers for improved energy consumption monitoring and customer billing was also reported in [21]. A reliable PLC system was designed in [22] to relay price and energy information to customers, enabling energy conservation benefits such as peak load shifting, shedding and automatic load controls. Reference [23] also achieves energy conservation via NB-PLC by broadcasting control commands to intelligent air conditioners. To the knowledge of the authors, most of the existing literature on the application of PLC in smart grids focuses on achieving high-data-rate communication. As a result, insufficient attention has been paid to exploring effective communication strategies for smart grid applications where reliability and coverage at low data rates are the primary concerns, especially in buildings with harmful attenuation levels.

III. QUASI-PEAK OPPORTUNITY

Typical high-speed PLC modems must limit their transmitted power to satisfy peak conducted emission limits. These devices cannot provide reliable wide-range PLC in challenging communication channels. However, for low-bandwidth communication applications, the regulatory limits on quasi-peak conducted emissions permit higher transmitted power levels.

Table I presents the NB-PLC conducted emissions limits enforced by some governing entities. The conducted EMI analysis presented here also extends to radiated EMI. NB-PLC conducted emissions limits expressed in dBμV are usually defined in terms of their peak (P), quasi-peak (QP) or average (AV) values. The NB-PLC conducted emissions limits defined by CENELEC in EN 50065-1 [13] are restricted to the 3–148.5-kHz range as shown in Table I. Only utility providers may use the 3–95-kHz range as dictated by EN 50065-1. General applications can make use of the 95-148.5-kHz band [13]. IEEE Std. 1901.2 recommends QP and AV emissions limits given in Table I for the unregulated 150–500-kHz band. This standard does not impose a P limit, and thus, this paper focuses on achieving robust and reliable low-data-rate NB-PLC in the 150–500-kHz frequency band by leveraging the opportunity provided by the QP limits and measurement procedure.

Fig. 1(a) shows the conducted EMI measurement set-up recommended in CISPR 16-1-1 [24]. This measurement set-up is currently employed by the FCC [14] and CENELEC [13] in the United States and Europe, respectively. A line impedance
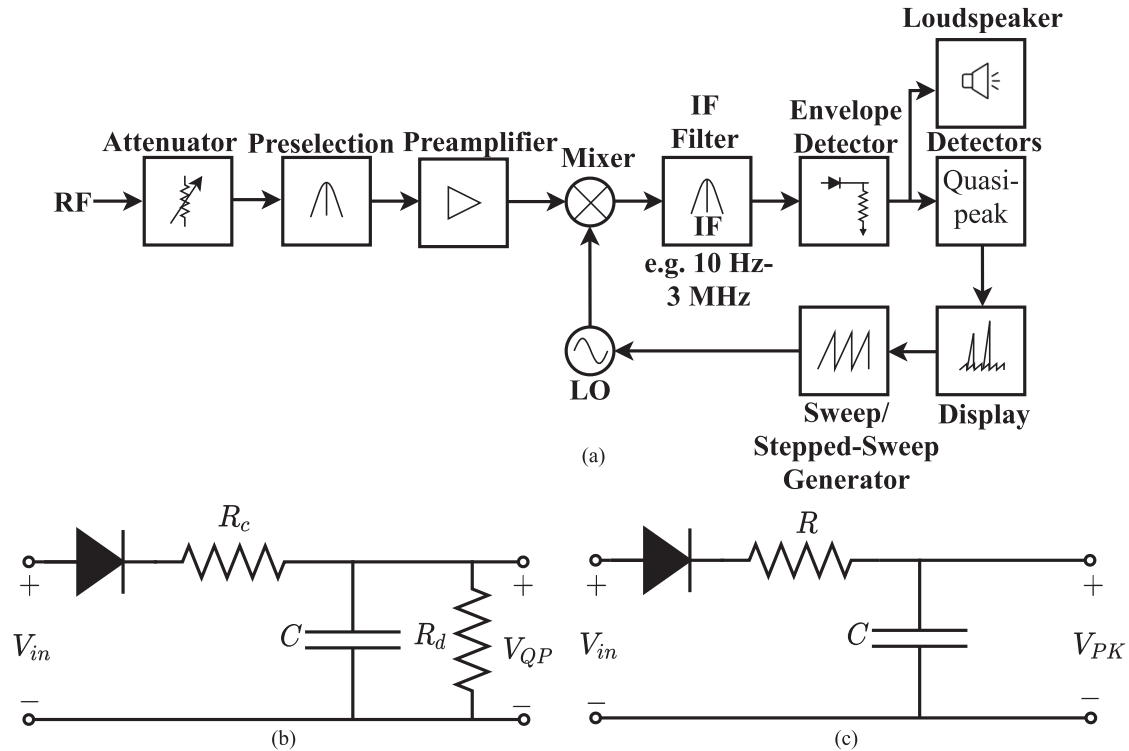
Fig. 1.   (a) Recommended CISPR conducted emissions measurement set-up. (b) Quasi-peak detector circuit. (c) Peak detector circuit.

stabilization network (LISN) is placed between the PLC device under test (DUT) and the EMI receiver shown in Fig. 1(a). The LISN presents a constant 50-Ω impedance to the DUT for high-frequency currents and blocks noise on the power line. The transmitted RF signal from the DUT is pre-conditioned before down-mixing to the baseband for further processing. A sweep or stepped-sweep generator sets the output of the local oscillator (LO) to cover the frequency range of interest designated by the EMC standard [24]. An intermediate frequency (IF) filter with a 6-dB bandwidth of 8-10 kHz filters the resulting signal. The center frequency of the IF filter can be between 10 Hz and 3 MHz [24]. Finally, the circuits in Figs. 1(b) and 1(c) generate the QP or P value of the signal's envelope respectively. These values are measured by a second-order critically-damped indicating instrument [24]. The circuit in Fig. 1(c) can also generate the AV value when the diode is replaced by a buffer. The resulting measurements vary depending on the structure and bandwidth of the input RF signal, and parameters of the IF filter and detectors.

Leveraging the QP regulatory limits to achieve high reliability in low-bandwidth PLC systems starts with examining the QP detector in more detail. The QP detector given in Fig. 1(b) is consistent with EMI testing standards defined by CISPR [15]. The QP detector circuit consists of a diode, a capacitor and two resistors as shown in Fig. 1. The capacitor voltage, V_{QP}, is the output of the QP detector and the diode prevents the capacitor from charging when V_{QP} is higher than V_{in}. When the envelope detector generates a pulse at V_{in}, it charges the capacitor through resistor R_c. When V_{in} is below V_{QP}, the capacitor discharges through resistor R_d. CISPR provides
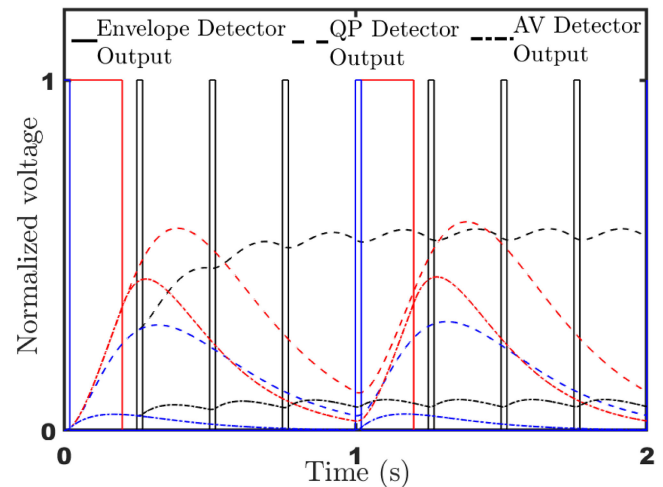

Fig. 2.   Impact of pulse width and period on the output of the QP and AV detectors.

the necessary charging and discharging time constants [24]. Given various RF input signals with equal amplitude, the QP detector will generate a lower QP value as either the signal's pulse width or pulse frequency decreases. Fig. 2 demonstrates this phenomenon by varying the pulse width and pulse frequency of a potential transmitted signal. PLC systems generally encode a data symbol in each transmission pulse, so the QP value will increase as the symbol rate increases. The AV value of a short pulse is usually significantly lower than the QP value as shown
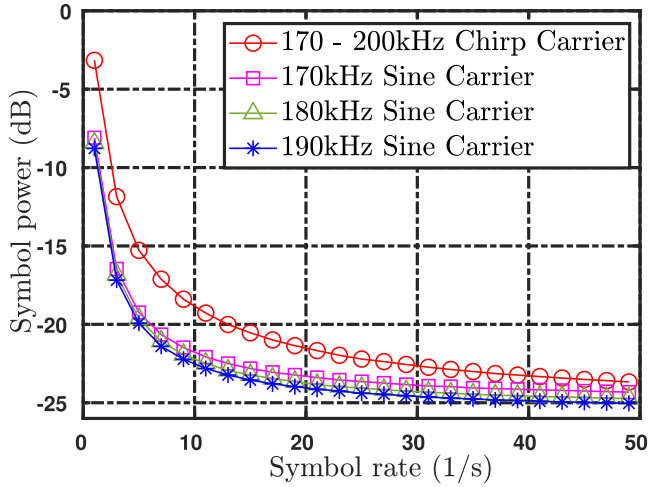
Fig. 3. Impact of quasi-peak limits on maximum transmitted power of various carrier signals when varying symbol rate.

Fig. 4. Impact of quasi-peak limits on maximum transmitted power of various carrier signals when varying pulse width.

in Fig. 2. Thus, the QP value is most often the limiting factor in maximum transmitted power.

The IF filter only allows the EMI receiver in Fig. 1(a) to capture energy within its pass band. Signals with larger bandwidths than the IF filter have a lower QP value than signals with a single carrier frequency. A chirp signal is one way to spread the spectral content partially outside the bandwidth of the IF filter. Instantaneously, the chirp signal is a single frequency that can pass through the IF filter during some part of the frequency sweep. The rate of the frequency sweep, combined with the bandwidth of the IF filter, sets the width of the pulse on the envelope detector output. Thus, a faster sweep rate reduces both the effective pulse width and the resulting QP value as shown in Fig. 2. When compared with a single carrier frequency signal, this wide-bandwidth chirp can achieve a lower QP value at frequencies common to both signals.

The EMI measurement procedure was simulated in MATLAB to determine the maximum allowable transmitted power for various NB-PLC carriers. Figs. 3 and 4 illustrate the impact of symbol rate, symbol width, and carrier type on the maximum achievable transmitted power. Fig. 3 shows that the maximum transmitted power per symbol increases as the symbol rate decreases, as long as the symbol width is held constant and the QP value is always at the limit. This effect is mainly driven by the discharge time of the QP detector. Fig. 4 demonstrates that maximum transmitted power per symbol increases as the width of the carrier pulse decreases. The nature of the QP detector creates this effect, and charging time determines what range of pulse widths permit higher power levels. Low-data-rate NB-PLC can utilize significantly higher transmitted power, and thus provides the best chance to achieve wide coverage and high reliability for smart grid PLC applications. The control of slow-switching heating, ventilation, and air-conditioning (HVAC) loads for demand-side management does not require high data throughput, and is an ideal application for low-data-rate NB-PLC.

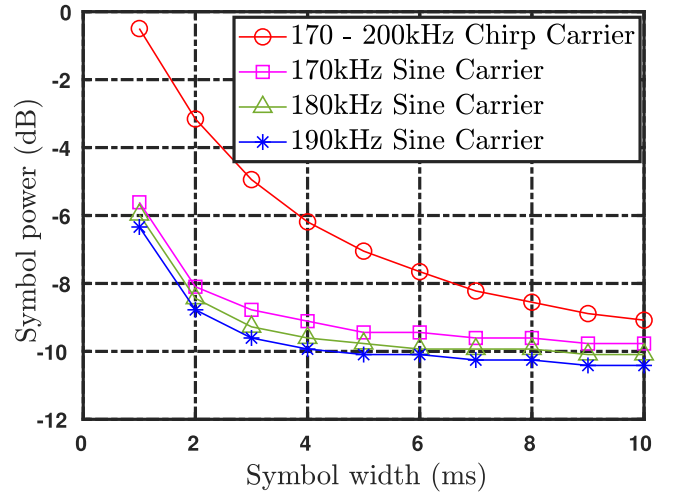The structure of the symbol carrier also impacts the transmitted symbol power. Frequency modulated carriers, with spectral content wider than the IF filter pass band, can transmit more power as shown in Figs. 3 and 4. The chirp signal is an easily customizable signal which leverages the characteristics of the EMI setup to operate at higher signal power. Thus, NB-PLC systems that encode data using signals similar to chirp signals can transmit more power per symbol than systems that employ single frequency carriers, such as binary phase shift keying or frequency shift keying (FSK). Although the injected signals used for Figs. 3 and 4 do not violate conducted emissions limits, safety limits such as surge voltage should be considered during system design.

IV. CHIRP SPREAD SPECTRUM

By spreading the carrier spectrum to occupy a wide range of the allocated frequency band, spread-spectrum communication can combat narrowband frequency-selective attenuation and multipath fading in PLC channels [25]. Direct-sequence [26], frequency-hopping [27], and chirp [28] are the most common spread-spectrum techniques. Chirp spread spectrum does not require accurate synchronization between the receiver and transmitter, which reduces the complexity of receiver circuits [29]. Chirp signals can encode each symbol into a wide frequency range. As discussed in Section III, this property allows for higher transmitted power and thus higher received power due to the properties of the EMI measurement setup.

A. Chirp Signal Theory

The time-domain representation of a chirp pulse waveform is

$$x(t) = A(t)\cos[\theta(t)] \qquad (1)$$

where $\theta(t)$ is the phase and $A(t)$ is the amplitude in the interval $0 \le t \le T$. T is the symbol duration. The instantaneous frequency, $f(t)$ is

$$f(t) = \frac{1}{2\pi}\frac{d\theta(t)}{dt} \qquad (2)$$

while the chirp rate, $\mu(t)$ is

$$\mu(t) = \frac{df(t)}{dt} = \frac{1}{2\pi}\frac{d^2\theta(t)}{dt^2}. \tag{3}$$

Chirp spread spectrum is achieved by spreading the instantaneous frequency, $f(t)$, across the frequency band of interest throughout the symbol duration. For linear chirps, $f(t)$ varies linearly with time and the chirp rate is constant.

This paper employs linear chirp signals that occupy part of the 150-500-kHz NB-PLC spectrum. The transmitted power increases as the bandwidth of the signal increases, and this property heavily affects the careful selection of chirp signal bandwidth. However, the higher frequency components of the carrier signal are more susceptible to PLC channel attenuation, and this effect limits the practical chirp signal bandwidth. This effect will be discussed in Section VI. When setting the bandwidth, the level of power transmitted and the fraction of power exposed to high levels of attenuation create a trade-off.

B. Proposed Modulation Scheme

This paper employs binary orthogonal keying (BOK) as the preferred modulation scheme. A digital bit "1" is encoded by a linear chirp signal with a positive chirp rate, $+|\mu|$. This is known as an "up-chirp". A "down-chirp" has a negative chirp rate, $-|\mu|$, and represents a digital bit "0". A "down-chirp" is represented by

$$x_0(t) = A_0(t)\cos[2\pi f_0 t - \pi|\mu|t^2 + \theta_0] \tag{4}$$

while an "up-chirp" is represented by

$$x_1(t) = A_1(t)\cos[2\pi f_1 t + \pi|\mu|t^2 + \theta_1]. \tag{5}$$

In (4) and (5), f_0 and f_1 are the frequencies at $t = 0$, θ_0 and θ_1 are the initial phases.

C. Proposed Receiver

The conventional receiver required to demodulate known signals in the presence of noise is discussed in chapter 6 of [30]. The receiver contains matched filters, envelope detectors, and threshold detectors. The proposed receiver's matched filters employed in this work are given by

$$g_i(t) = \int_0^T h_i(t-\tau)r(\tau)d\tau, \qquad 0 < t < T \tag{6}$$

where $i = 0, 1$ corresponds to the received "down-chirp" and "up-chirp" signals respectively. The impulse responses of the "down-chirp" and "up-chirp" are, respectively, given by

$$h_0(t) = x_0(T-t) = x_1(t) \tag{7}$$

and

$$h_1(t) = x_1(T-t) = x_0(t). \tag{8}$$

The received signal, $r(t)$, is

$$r(t) = \alpha(t)x_i(t) + n(t) \tag{9}$$

if a transmitted symbol is present or

$$r(t) = n(t) \tag{10}$$

if absent, where $n(t)$ is band-limited noise and $\alpha(t)$ is the channel gain. Due to the infrequent transmission of carrier signals required in low-bandwidth control and sensing applications, the absent-signal case must be considered.

This paper proposes a pseudo-binary receiver to determine the presence of $x_i(t)$ in $r(t)$. The envelope peaks of $g_0(t)$ and $g_1(t)$ are computed and compared to thresholds derived in Reference [30] to completely demodulate the received signal. Assuming equal energy in $x_0(t)$ and $x_1(t)$, the received bit is determined by the proposed receiver to be "1" if

$$\overline{g_1(t)} - \overline{g_0(t)} > \frac{N_0}{2}ln\left(\frac{P_0}{P_1}\right) \tag{11}$$

and

$$\overline{g_1(t)} > \frac{1}{2}\int_0^T x_1^2(t) + \frac{N_0}{2}ln\left(\frac{P_2}{P_1}\right) \tag{12}$$

are satisfied. In these conditions, $\overline{g_i(t)}$ denotes the peak of the i-th matched filter's output envelope and N_0 is the noise power. P_i is the *a priori* probability corresponding to (9) and P_2 is the *a priori* probability corresponding to (10).

Conversely, the received bit is determined to be "0" if

$$\overline{g_0(t)} - \overline{g_1(t)} > \frac{N_0}{2}ln(\frac{P_1}{P_0}) \tag{13}$$

and

$$\overline{g_0(t)} > \frac{1}{2}\int_0^T x_0^2(t) + \frac{N_0}{2}ln(\frac{P_2}{P_0}) \tag{14}$$

are satisfied. Otherwise, $r(t) = n(t)$ is said to be correct.

V. PROPOSED HARDWARE DESCRIPTION

The proposed PLC modem consists of both a transmitter and receiver, which interface with the electric utility through a shared multi-input and multi-output (MIMO) coupler. The design utilizes a Cypress PSoC 5LP microcontroller (MCU). The MCU is a mixed-domain chip that can implement configurable filters and mixers, in addition to performing analog-to-digital and digital-to-analog conversions. Fig. 5 presents the block diagram of the proposed PLC transmitter. A Tx stack buffer in the MCU stores the bit to be transmitted. The utility voltage provides a global clock to improve synchronization between different PLC modems. A zero-crossing detector implemented with an optoisolator converts the line voltage to a digital voltage-polarity signal. A monostable multivibrator in the MCU triggers on the rising edge of the zero-crossing detector's output, signaling the Tx stack buffer to "pop" the next bit for transmission. A switch temporarily blocks the signal from the monostable multivibrator after each transmission, limiting the data rate to $1/T_D$. The MCU modulates the bit from the Tx buffer into an 8-bit discrete-time chirp signal, and then performs digital-to-analog conversion (DAC). A switch in the MCU and the MIMO coupler's configuration determine the physical PLC channel. The chirp signal is conditioned in the analog front end by the programmable-gain amplifier (PGA), low-pass filter (LPF), and power amplifier (PA) before it reaches the coupler. The transformers and capacitors isolate the low-voltage circuitry from the high-voltage power
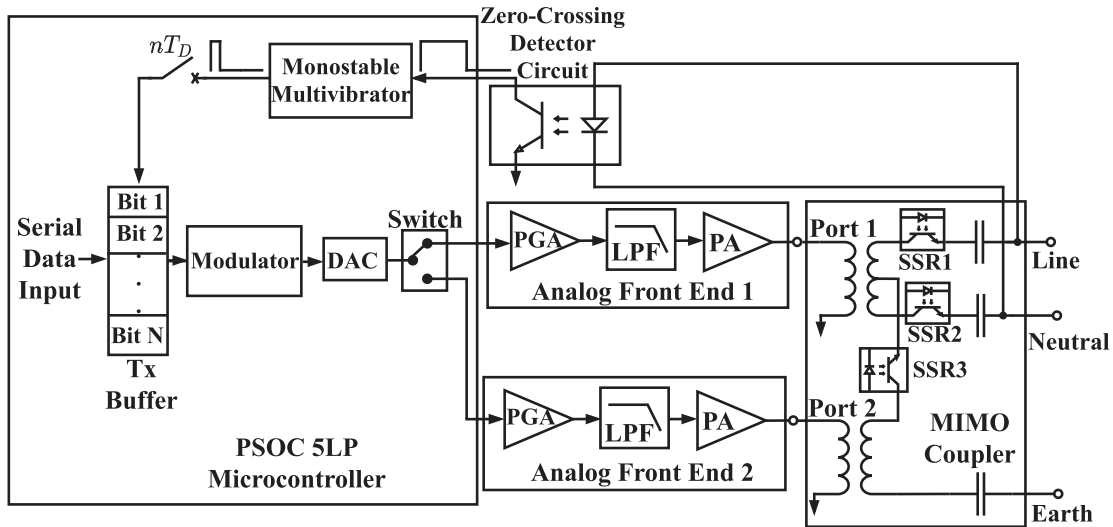
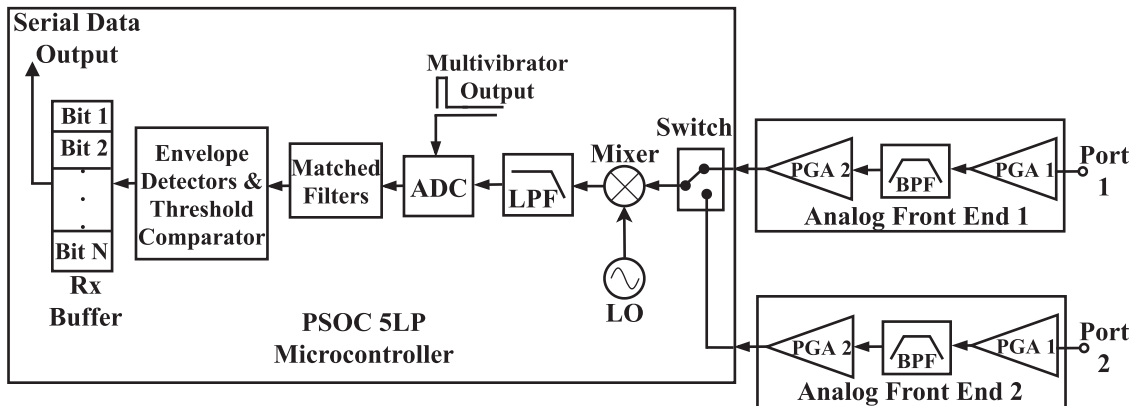Fig. 5.   Block diagram of the PLC modem transmitter.

Fig. 6.   Block diagram of the PLC modem receiver.

line. Solid-state relays (SSRs) change the connection of the coupler to the electric utility, affecting the physical PLC channel. For instance, when only SSR1 and SSR2 are ON, the line-neutral channel is being used. These circuit elements work together to inject a chirp signal current, which encodes a single bit, into the electric utility. After signal attenuation and corruption by noise, the receiver demodulates the received signal.

The receiver section of the proposed PLC modem is shown in Fig. 6. The corrupted signal passes through the MIMO coupler and into the analog front end. This front end condtions the received signal using PGAs and a band-pass filter. Similar to the transmitter, a switch in the MCU and the SSRs in the MIMO coupler determine the physical PLC channel. The resulting signal is down-mixed to baseband in the MCU. The LO frequency is determined by the maximum frequency of the chirp carrier signal. An LPF prevents aliasing in the sampling stage, and the cut-off frequency depends on the bandwidth of the chirp signal. An analog-to-digital converter (ADC), triggered by the same multivibrator in the transmitter, converts the received signal to its discrete-time form. This discrete-time received signal is the

input to the two matched filters presented in Section IV, which are implemented in discrete time. The envelope detectors and threshold comparator perform the operations given in (11)–(14) to determine the received bit. The Rx buffer stores the received bit to complete the demodulation process.

VI. EXPERIMENTAL TEST SYSTEM

To demonstrate the effectiveness of the proposed chirp spread-spectrum technique and PLC modem, a difficult electrical environment for PLC is selected. Here, a 24-floor high-rise building in the Massachusetts Institute of Technology (MIT) campus is used. The building has challenging attenuation characteristics and provides an excellent testing ground for the proposed PLC technique and hardware.

The electrical system of the test building is shown in Fig. 7. Power is delivered from the grid through a three-phase delta-wye grounded transformer located in the basement of the building. The main service panel consists of an air circuit breaker fed from the transformer by three-phase four-wire cabling. The neutral
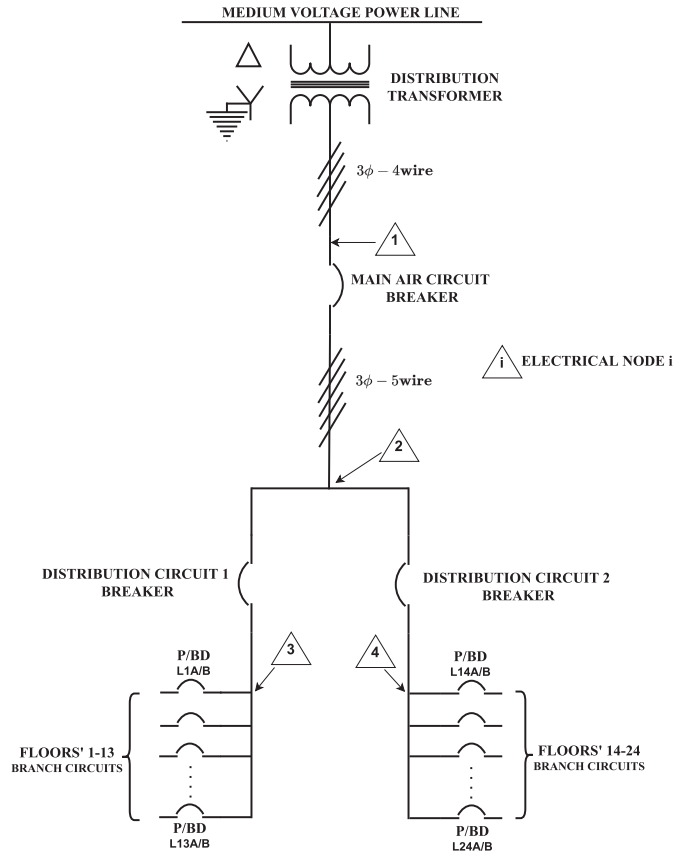
Fig. 7.   Electrical circuit diagram of a 24-floor high-rise apartment building on MIT campus.
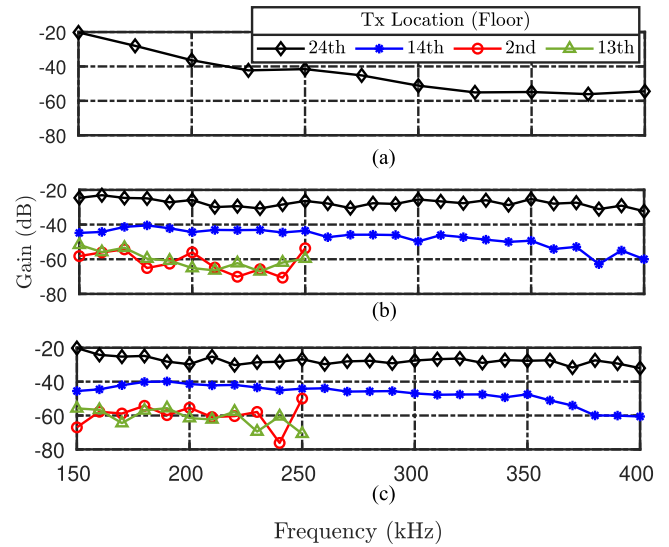

Fig. 8.   Channel gain of key communication links in the test building with PLC receiver on 24th floor. (a) line-neutral channel. (b) neutral-earth channel. (c) line-earth channel.

and earth are bonded together at node 1 in Fig. 7. The out-going three-phase five-wire cabling splits at node 2 to supply the two main circuits in the building. The building is electrically divided into two groups. Floors one to thirteen are supplied from one main circuit, while fourteen through twenty-four are supplied from the other as indicated in Fig. 7. The main circuits branch out at nodes 3 and 4. Each floor is protected by two circuit breakers in addition to distribution breakers for each main circuit. The three-phase, five-wire supply cables are divided at each floor's branch circuit to carry single-phase power to the numerous single-phase power outlets on each floor. The only exceptions are the 208 V phase-phase power outlets for electric ovens in the residences. As a result, some single-phase power outlets on the same floor are supplied from different phases of the three-phase distribution circuits. In general, results published in [9] show that PLC performance does not degrade significantly when communicating from one phase to another.

Consider a building automation/smart-grid application relying on PLC installed in this building. Controllable loads, such as HVACs and dishwashers, are fitted with PLC modems and connect to different branch circuits located on various floors in the high-rise building. The array of utility connections forms a local communication network. The size and structure of the building's power distribution network increases network complexity and places varying electrical distance between different modems.

Depending on the location of two communicating PLC modems, signals must pass through multiple circuit breakers, EMI chokes, and filters. These elements introduce extra obstacles that are not usually present in smaller residential buildings. This typically translates to higher signal attenuation between transmitting and receiving nodes [9].

To evaluate the attenuation characteristics of the test building, a receiver is placed on the 24th floor, and a transmitter is placed on the 2nd, 13th, 14th, or 24th floor. Fig. 8 presents the attenuation results for the various transmitter locations and utility connections. The results in Fig. 8 are employed to select appropriate physical and spectral PLC channels in this work. A more sophisticated channel selection process that uses impedance information at the transmitter, noise information at the receiver and attenuation will be presented in a future paper. The MIMO coupler of the PLC modem transmitter shown in Fig. 5 is configured as discussed in Section V to probe the individual physical channels. The main components of the MIMO coupler are one center-tapped and one non-center-tapped PLC transformers manufactured by Wurth Electronics. It also consists of three 0.15 μF metalized polypropylene capacitors rated at 300VAC and three solid-state relays already mentioned in Section V.

The attenuation of the 24th to 24th floor line-neutral channel is shown in Fig. 8(a). The attenuation varies from about 20 dB at 150 kHz to 56 dB at 375 kHz. Due to excessive signal attenuation on the line-neutral channel, the attenuation could not be accurately estimated for the other transmitter locations. Signal attenuation on the neutral-earth and line-earth channels are presented in Figs. 8(b) and 8(c) respectively. The attenuation on the 2nd to 24th and 13th to 24th floor links could not be accurately estimated at frequencies greater than 250 kHz and is not reported. Figs. 8(b) and (c) show that the neutral-earth and line-earth channel attenuation is lower than the line-neutral

channel attenuation. The presence of power electronics EMI filters introduces a significantly higher capacitive load on the line to neutral channel. This is the major reason the attenuation on the line to neutral channel is significantly larger than the attenuation on the other channels. Figs. 8(b) and (c) also reveal that moving the transmitter from the 24th to the 14th floor increases the attenuation by about 15 dB on average. However, when the transmitter is moved by one more floor (14th to 13th), the average attenuation increases by an additional 25 dB. The 13th floor is on a different distribution circuit than the 14th and 24th floors, resulting in the rapid increase in attenuation. Communication signals experience more attenuation in this case because they travel a longer distance and through more breakers as indicated in Fig. 7. The attenuation in the 2nd and 13th to 24th floor links are very similar because both transmitting floors are on the same circuit and signal degradation is dominated by crossing from one circuit to the other. NB-PLC attenuation in the test building is about 10–50 dB greater than the attenuation recorded in other buildings presented in [6] and [9]. Despite the above-average challenges of this building's PLC channels, the proposed technique and hardware can achieve reliable low-data-rate PLC.

VII. EXPERIMENTAL RESULTS AND DISCUSSION

Now that the test environment has been characterized, the data transmission performance of the proposed low-data-rate PLC technique and hardware can be evaluated. Other modulation schemes, including chirp-BOK and FSK, are also evaluated to show the benefit of the chirp technique when operating at the QP regulatory limit.

In these tests, a transmitting PLC modem is connected to the electric utility on various floors of the test building. The modem's Tx buffer is loaded with a known symbol (bit) sequence to evaluate the detection probability. The receiver modem is connected to the electric utility on the 24th floor and will attempt to decode the transmitted bit sequence. The rates and power levels of various symbols are used to measure the transmitted symbol detection probability as a function of symbol rate or signal-to-noise ratio (SNR). To minimize attenuation as shown in Fig. 8, the line-earth physical channel and 170–200-kHz spectral channel are used. Consequently, linear chirps with 30-kHz bandwidth and 4 ms duration are employed to modulate the digital data. The receiver's ADC sampling frequency is set to 1 MSps, the receiver LO frequency is 210 kHz, and the anti-aliasing filter cut-off frequency is 45 kHz.

A. Performance of the Proposed Communication Scheme

Fig. 9 provides an overview of communication performance using BOK modulation at the QP regulatory limit. The probability of successfully detecting a symbol is plotted against symbol rate with the transmitter placed on either the 2nd, 9th, 13th, 14th, or 24th floor. The PLC modems maintain high fidelity communication when the transmitter and receiver are on the same distribution circuit, i.e., when the transmitter is placed on the 14th or 24th floor. One-hundred percent reliable communication is possible at up to 8 symbols-per-second. In contrast, the PLC modems placed on the 2nd, 9th, and 13th floors drop below
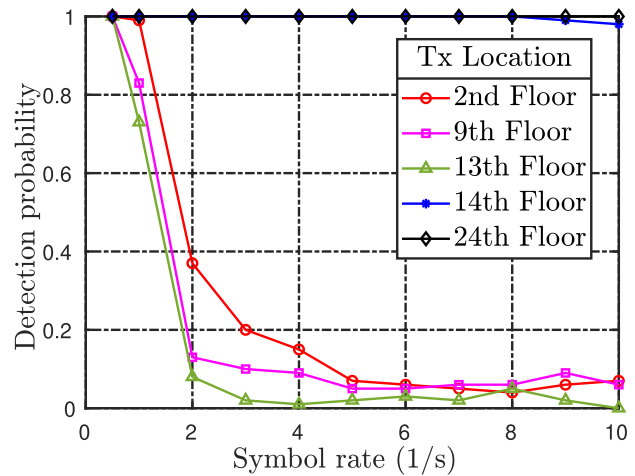

Fig. 9. Impact of chirp-BOK modulation at the QP regulatory limit on PLC performance in the test building.

50% reliability at 2 symbols-per-second. As Fig. 8 demonstrated, communication between the two main distribution circuits in the test building results in heavy attenuation, leading to weak performance PLC. However, the reliability typically remains above 0%, allowing techniques at the data transport layer to make use of the PLC link for low-data-rate applications.

Smart grid applications, such as load control and demand response, depend on coverage and reliability rather than communication bandwidth. The proposed technique and hardware meet this challenge by enabling low-data-rate PLC in extremely harsh electrical environments.

B. Impact of Leveraging QP Regulation Opportunity

The QP opportunity permits higher transmission power, but only in the absence of a P limit. The QP technique presented in Section III leverages the measurement circuit to maximize the signal energy for each symbol. Without a P limit, the QP limit values may be used as a substitute, leading a designer to reduce the power level unnecessarily. The resulting PLC modems will have lower reliability and coverage. Fig. 10 demonstrates this effect by displaying new 2nd and 14th floor tests with the the transmitter peak power equal to the QP limit. Fig. 10 shows the reduced communication reliability resulting from lower transmission power. The detection probability from the 14th floor drops by 40–50% across the measured symbol-rate range. In the 2nd floor case, the probability drops by as much as 90%. Thus, leveraging the QP opportunity is necessary to maximize the coverage and reliability of low-data-rate PLC modems.

C. Modulation Scheme Comparison

The chirp signal better utilizes the QP opportunity by interacting with the IF filter to shorten the measured pulse width. A single frequency carrier scheme, such as FSK, does not have this advantage and must transmit at lower power for the same pulse width. Fig. 11 demonstrates the disadvantage posed by FSK. Here, 170-kHz and 180-kHz sinusoidal carriers represent "1"
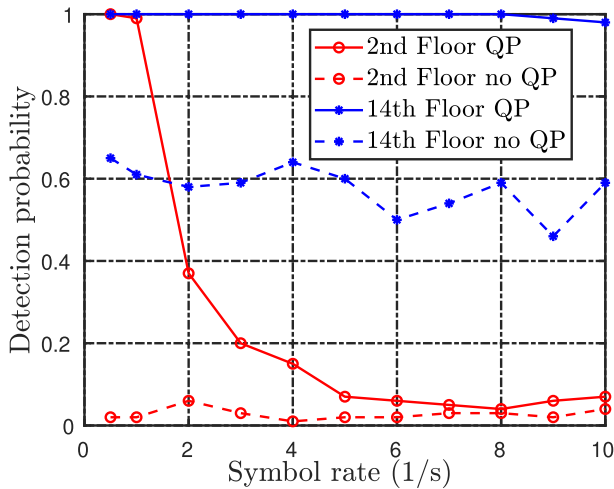
Fig. 10.   Effect of leveraging QP regulations on chirp-BOK modulation scheme performance.
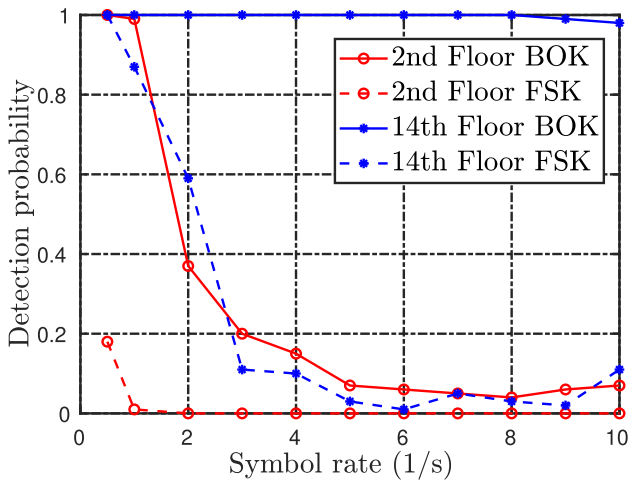

Fig. 12.   Proposed receiver operating characteristics showing the impact of matched filter's output SNR on symbol detection rate.

Fig. 11.   Performance comparison between chirp-BOK and FSK modulation schemes.

fit with an exponential function. The ROC allows a PLC system designer to estimate the performance of PLC modems based on known channel characteristics and transmission power. The ROC permits estimation of performance when error-correction codes (ECC) are employed.

VIII. CONCLUSION

The proposed leveraging of the QP measurement technique, combined with chirp-BOK modulation, permits dramatically improved reliability and coverage for PLC modems. Smart-grid applications, such as load control and demand response, can take advantage of the enhanced coverage without being limited by the low data rate. This article presents an experimental case study in a high-rise building with challenging PLC channel characteristics to demonstrate the performance of the proposed PLC modem. Experiments also demonstrate the benefit of chirp-BOK modulation in comparison to FSK to better utilize the QP regulatory limit.

and "0" respectively. Again, the transmitter is placed on either the 2nd or 14th floor for these tests. In either case, the FSK performance is dramatically lower than the proposed chirp-BOK technique. In the 2nd floor case, the reliability drops by as much as 95%. Further, a FSK-based PLC link cannot be established at or above 2 symbols-per-second. This test demonstrates that the proposed BOK modulation scheme improves communication fidelity compared to FSK by permitting higher transmitted power levels.

D. Proposed Receiver Operating Characteristics

The receiver operating characteristics (ROC) indicate the reliability of a receiver with respect to SNR. Fig. 12 gives the ROC of the proposed PLC modem when utilizing the full QP opportunity with chirp-BOK modulation. The curve utilizes the data collected for various transmitter locations. The SNR is calculated from the output of the matched filter. The plot also gives a curve
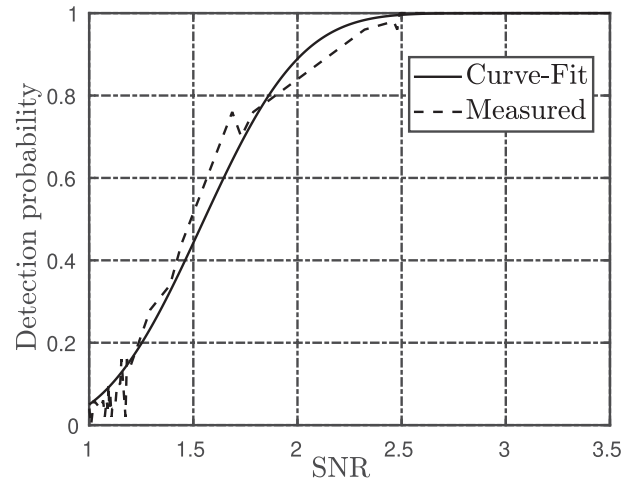
REFERENCES

[1] S. C. Shabshab et al., "Demand smoothing in military microgrids through coordinated direct load control," IEEE Trans. Smart Grid, vol. 11, no. 3, pp. 1917–1927, May 2020.

[2] M. Nassar, J. Lin, Y. Mortazavi, A. Dabak, I. H. Kim, and B. L. Evans, "Local utility power line communications in the 3–500 kHz band: Channel impairments, noise, and standards," IEEE Signal Process. Mag., vol. 29, no. 5, pp. 116–127, Sep. 2012.

[3] S. Galli, A. Scaglione, and Z. Wang, "For the grid and through the grid: The role of power line communications in the smart grid," Proc. IEEE, vol. 99, no. 6, pp. 998–1027, Jun. 2011.

[4] H. Farhangi, "The path of the smart grid," IEEE Power Energy Mag., vol. 8, no. 1, pp. 18–28, Jan./Feb. 2010.

[5] C. Cano, A. Pittolo, D. Malone, L. Lampe, A. M. Tonello, and A. G. Dabak, "State of the art in power line communications: From the applications to the medium," IEEE J. Sel. Areas Commun., vol. 34, no. 7, pp. 1935–1952, Jul. 2016.

[6] K. Sharma and L. M. Saini, "Power line communications for smart grid: Progress, challenges, opportunities and status," Renewable Sustain. Energy Rev., vol. 67, pp. 704–751, 2017.

[7] N. Pavlidou, A. J. H. Vinck, J. Yazdani, and B. Honary, "Power line communications: State of the art and future trends," *IEEE Commun. Mag.*, vol. 41, no. 4, pp. 34–40, Apr. 2003.

[8] R. M. Vines, H. J. Trissell, L. J. Gale, and J. B. O'neal, "Noise on residential power distribution circuits," *IEEE Trans. Electromagn. Compat.*, vol. EMC-26, no. 4, pp. 161–168, Nov. 1984.

[9] M. H. L. Chan and R. W. Donaldson, "Attenuation of communication signals on residential and commercial intrabuilding power-distribution circuits," *IEEE Trans. Electromagn. Compat.*, vol. 28, no. 4, pp. 220–230, Nov. 1986.

[10] M. Zimmermann and K. Dostert, "A multipath model for the powerline channel," *IEEE Trans. Commun.*, vol. 50, no. 4, pp. 553–559, Apr. 2002.

[11] R. M. Vines, H. J. Trussell, K. C. Shuey, and J. B. O'Neal, "Impedance of the residential power-distribution circuit," *IEEE Trans. Electromagn. Compat.*, vol. EMC-27, no. 1, pp. 6–12, Feb. 1985.

[12] M. Girotto and A. M. Tonello, "EMC regulations and spectral constraints for multicarrier modulation in PLC," *IEEE Access*, vol. 5, pp. 4954–4966, 2017.

[13] *Signaling on Low Voltage Electrical Installations in the Frequency Range 3 kHz to 148.5 kHz, Part 1: General Requirements, Frequency Bands and Electromagnetic Disturbancesbibpunc*, European Committee for Electrotechnical Standardization, CENELEC, EN50065-1, 2001.

[14] *Radio Frequency Devices*. Electronic Code of Federal Regulations, Jul. 2008. [Online]. Available: http://www.fcc.gov/oet/info/rules/part15.pdf

[15] CISPR, "22: Information technology equipment radio disturbance characteristics limits and methods of measurement IEC," 2005.

[16] *IEEE Standard for Low-Frequency (Less than 500 kHz) Narrowband Power Line Communications for Smart Grid Applications*, IEEE Standard 1901.2-2013, 2013, pp. 1–269.

[17] *IEEE Recommended Practice and Requirements for Harmonic Control in Electric Power Systems*, IEEE Standard 519-2014 (Revision of IEEE Standard 519-1992), 2014, pp. 1–29.

[18] *IEEE Recommended Practice on Characterization of Surges in Low-Voltage (1000 V and Less) AC Power Circuits*, IEEE Standard C62.41.2-2002, 2003, pp. 1–53.

[19] T. IEC, "60755: Residual current protective device dependent or independent in line voltage," 2008.

[20] D. P. F. Möller and H. Vakilzadian, "Ubiquitous networks: Power line communication and Internet of Things in smart home environments," in *Proc. IEEE Int. Conf. Electron./Inf. Technol.*, 2014, pp. 596–601.

[21] J. Matanza, S. Alexandres, and C. Rodríguez-Morcillo, "Advanced metering infrastructure performance using european low-voltage power line communication networks," *IET Commun.*, vol. 8, no. 7, pp. 1041–1047, May 2014.

[22] Y. Chen and J. K. Hwang, "A reliable energy information system for promoting voluntary energy conservation benefits," *IEEE Trans. Power Del.*, vol. 21, no. 1, pp. 102–107, Jan. 2006.

[23] S. Hsieh, T. Ku, C. Chen, C. Lin, and J. Tsai, "Broadcasting control of intelligent air conditioners using power-line-carrier technology," *IEEE Trans. Ind. Appl.*, vol. 51, no. 2, pp. 1890–1896, Mar./Apr. 2015.

[24] *Specification for Radio Disturbance and Immunity Measuring Apparatus and Methods-Part 1-1: Radio Disturbance and Immunity Measuring Apparatus-Measuring Apparatus*, International Electrotechnical Commission, IEC, CISPR 16-1-1, 2015.

[25] H. Dai and H. V. Poor, "Advanced signal processing for power line communications," *IEEE Commun. Mag.*, vol. 41, no. 5, pp. 100–107, May 2003.

[26] P. van der Gracht and R. Donaldson, "Communication using pseudonoise modulation on electric power distribution circuits," *IEEE Trans. Commun.*, vol. 33, no. 9, pp. 964–974, Sep. 1985.

[27] K. M. Dostert, "Frequency-hopping spread-spectrum modulation for digital communications over electrical power lines," *IEEE J. Sel. Areas Commun.*, vol. 8, no. 4, pp. 700–710, May 1990.

[28] D. Kim, S. Lee, K. Wang, J. Choi, and D. Chung, "A power line communication modem based on adaptively received signal detection for networked home appliances," *IEEE Trans. Consum. Electron.*, vol. 53, no. 3, pp. 864–870, Aug. 2007.

[29] D. Radford, "Spread spectrum data leap through AC power wiring," *IEEE Spectr.*, vol. 33, no. 11, pp. 48–53, Nov. 1996.

[30] A. D. Whalen, *Detection of Signals in Noise*, 2nd ed. San Diego, CA, USA: Academic Press, 2013.

Adedayo O. Aderibole received the B.Sc. degree in electronic or electrical engineering from Obafemi Awolowo University, Ile-Ife, Nigeria, in 2013, and the M.Sc. degree in electrical power engineering from Masdar Institute, Khalifa University of Science and Technology, Abu Dhabi, United Arab Emirates, in 2017. He is currently working toward the Ph.D. degree in electrical engineering and computer science with the Massachusetts Institute of Technology, Cambridge, MA, USA. His research interests include communication theory, signal processing, and power system modeling and control.

Erik K. Saathoff (Graduate Student Member, IEEE) received the B.S. degree in electrical engineering with a minor in physics from the University of Illinois at Urbana-Champaign, Urbana, IL, USA, and in 2018, the M.S. degree in 2021 in electrical engineering and computer science from the Massachusetts Institute of Technology, Cambridge, MA, USA, where he is currently working toward the Ph.D. degree in electrical engineering and computer science. His research interests include high-performance power electronics, switched-capacitor converters, and system identification.

Kevin J. Kircher received the Ph.D. degree in mechanical engineering from Cornell University, Ithaca, NY, USA, in 2019. He is currently a Postdoctoral Researcher of electrical engineering and computer science with the Massachusetts Institute of Technology, Cambridge, MA, USA. His research interests include learning, optimization, and control methods to smart buildings and their interaction with the electrical grid.

Steven B. Leeb (Fellow, IEEE) received the Ph.D. degree from the Massachusetts Institute of Technology, Cambridge, MA, USA, in 1993. He was a Commissioned Officer with the USAF reserves, and he has been a Member of the M.I.T. Faculty with the Department of Electrical Engineering and Computer Science since 1993. He also holds a joint appointment in MIT's Department of Mechanical Engineering. He is the Author or Co-Author of more than 200 publications and 20 U.S. patents in the fields of electromechanics and power electronics.

Leslie K. Norford received the Ph.D. degree in mechanical and aerospace engineering from Princeton University, Princeton, NJ, USA, in 1984, after five years of active duty as a nuclear power officer in the US Navy. Since 1988, he has been a Member with the Faculty of the Department of Architecture, Massachusetts Institute of Technology, Cambridge, MA, USA. His research interests include design, operation, and fault detection of space conditioning systems for low-carbon buildings and interactions of buildings with the electrical grid and with urban environments.